Journal Pre-proofs


# Development of a PAT platform for the prediction of granule tableting properties

Tibor Casian, Brigitta Nagy, Cristiana Lazurca, Victor Marcu, Erzsébet Orsolya Tőkés, Éva Katalin Kelemen, Katalin Zöldi, Radu Oprean, Zsombor Kristóf Nagy, Ioan Tomuta, Béla Kovács

PII: S0378-5173(23)01031-1
DOI: https://doi.org/10.1016/j.ijpharm.2023.123610
Reference: IJP 123610

To appear in: *International Journal of Pharmaceutics*

Received Date: 4 September 2023
Revised Date: 26 October 2023
Accepted Date: 14 November 2023

Please cite this article as: T. Casian, B. Nagy, C. Lazurca, V. Marcu, E. Orsolya Tőkés, E. Katalin Kelemen, K. Zöldi, R. Oprean, Z. Kristóf Nagy, I. Tomuta, B. Kovács, Development of a PAT platform for the prediction of granule tableting properties, *International Journal of Pharmaceutics* (2023), doi: https://doi.org/10.1016/j.ijpharm.2023.123610

# Development of a PAT platform for the prediction of granule tableting properties

Tibor Casian [a], Brigitta Nagy [b,*], Cristiana Lazurca [a], Victor Marcu [a], Erzsébet Orsolya Tőkés [c], Éva Katalin Kelemen [c], Katalin Zöldi [c], Radu Oprean [d], Zsombor Kristóf Nagy [b], Ioan Tomuta [a], Béla Kovács [c,e]

[a]

Department of Pharmaceutical Technology and Biopharmacy, "Iuliu Hatieganu" University of Medicine and Pharmacy, 400012 Cluj-Napoca, Romania

[b]

Department of Organic Chemistry and Technology, Faculty of Chemical Technology and Biotechnology, Budapest University of Technology and Economics, Műegyetem rkp. 3., H-1111 Budapest, Hungary

[c]

Gedeon Richter Romania 540306, Tîrgu Mureș, Romania

[d]

Analytical Chemistry Department, "Iuliu Haţieganu" University of Medicine and Pharmacy, 400349, Cluj-Napoca, Romania

[e]

Department of Biochemistry and Environmental Chemistry, Faculty of Pharmacy, George Emil Palade University of Medicine, Pharmacy, Science, and Technology of Târgu Mureș, 540139 Târgu Mureș, Romania

*corresponding author: nagy.brigitta@vbk.bme.hu; Tel.: +36-1-463-1111/5918

Abstract

In this work, the feasibility of implementing a process analytical technology (PAT) platform consisting of Near Infrared Spectroscopy (NIR) and particle size distribution (PSD) analysis was evaluated for the prediction of granule downstream processability. A Design of Experiments-based calibration set was prepared using a fluid bed melt granulation process by varying the binder content, granulation time, and granulation temperature. The granule samples were characterized using PAT tools and a compaction simulator in the 100-500kg load range. Comparing the systematic variability in NIR and PSD data, their complementarity was demonstrated by identifying joint and unique sources of variation. These particularities of the data explained some differences in the performance of individual models. Regarding the fusion of data sources, the input data structure for partial least squares (PLS) based models did not significantly impact the predictive performance, as the root mean squared error of prediction (RMSEP) values were similar. Comparing PLS and artificial neural network (ANN) models, it was observed that the ANNs systematically provided superior model performance. For example, the best tensile strength, ejection stress, and detachment stress prediction with ANN resulted in an RMSEP of 0.119, 0.256, and 0.293 as opposed to the 0.180, 0.395, and 0.430 RMSEPs of the PLS models, respectively. Finally, the robustness of the developed models was assessed.

Highlights

- NIR and granule size distribution data were fused to predict tableting properties.
- ANN-based modeling offered an improved performance compared to PLS.
- Tabletability and stress values during tablet detachment/ejection were predicted.

Keywords

Near Infra-red spectroscopy, Data fusion, Artificial neural networks, Granules, Tabletability, PAT

## 1. Introduction

The applied quality management strategies have evolved over time to compensate for the multivariate nature of drug manufacturing. The highest level of quality management that is considered to revolutionize industrial manufacturing of medicine relies on the use of soft sensors that can enable the future of smart manufacturing in a Quality by Control (QbC) environment (Jelsch et al., 2021; Mathe et al., 2020). In this respect, Process Analytical Technology (PAT) is of central importance to achieving model predictive control, by continuously measuring critical quality attributes (CQAs) (Casian et al., 2019b).

Tableting is an important production process in the pharmaceutical industry due to its high output, cost-effectiveness, and economic benefits. However, the process highly depends on the product properties and the manufacturing conditions (Kalies et al., 2020). Despite being the most common pharmaceutical dosage form, the appearance of tablet quality variations during the product's life cycle is typical and can be linked to multiple factors, e.g., variable critical material attributes and processing conditions, supplier changes, equipment wear (Mazel et al., 2019, 2015; Paul and Sun, 2017). Thus, proper control of the tableting step should also consider implementing process analytical tools capable of evaluating the tableting properties of intermediate products. Such tools could be used efficiently for the implementation of a feed-forward or feed-back process control strategy, especially in the context of a continuous manufacturing setup (Domokos et al., 2021; Madarász et al., 2022, 2020; Záhonyi et al., 2023).

Pharmaceutical granulation is an essential step in manufacturing solid oral dosage forms that is applied to increase the tableting properties and flowability of the powder blend (Casian et al., 2022a; Gavan et al., 2020; Mathe et al., 2020). Considering this step's multivariate nature and complexity, appropriate control of critical material attributes (CMAs), external factors, and critical process parameters (CPPs) is required to avoid CQA variations and downstream processing issues. In a previous work, we demonstrated how these factors' slight but combined variation could impact product performance at the industrial scale (Mathe et al., 2020). To ensure improved knowledge, individual PAT tools have been implemented to provide understanding of flowing (Alam et al., 2017) and lubrication properties (Blanco et al., 2021), that can have an impact on mass variation (Mathe et al., 2020) or the sticking tendency of tablets (Saddik and Dave, 2021); heat transfer during drying (Domokos et al., 2021) as the drying profile impact downstream processability(Mathe et al., 2020); respectively particle size and size distribution (Porfire et al., 2012) as it can impact compressibility and compactibility during tableting (Wünsch et al., 2021). Although these approaches have well-demonstrated utility, a more comprehensive approach is required for improved and more robust quality control.

Predicting tabletability is a critical step in tablet manufacturing because it allows for adjustments before issues arise during large-scale production, such as capping, lamination, friability, etc. (Mazel and Tchoreloff, 2022). The combination of analytical techniques, physical testing, computational models (Hattori et al., 2020), and advanced data analytics (De Bisshop and Klinken, 2023; Jin et al., 2022) contributes to accurate tabletability prediction, ultimately leading to the production of high-quality tablets.

Hattori et al. have developed a robust feed-forward control model that predicts process parameters of tablet compression by leveraging the chemical (NIR spectra) and physical characteristics ( particle size distribution - PSD, bulk and tapped density, flowability) of the granules (Hattori et al., 2020). Non-destructive spectrometric techniques can provide real-time information about the chemical and physical properties of granules or powder blends used in tablet production, which are critical for predicting tabletability. PSD has been extensively

studied in various technological processes, and it stands as one of the most crucial factors impacting tablet Critical Quality Attributes (CQAs) (Pauli et al., 2019). For instance, as shown by Skelbæk-Pedersen et al., insufficient particle size control can lead to undesired tablet fragmentation, resulting in suboptimal tablet compression. They measured the extent of fragmentation in various deforming materials with differing initial particle sizes, relying on the PSD of compressed particles and employing NIR spectroscopy as a substitute technique for examining fragmentation. NIR spectroscopy has demonstrated its potential as a valuable tool for examining subtle variations in particle size within limited PSDs and for evaluating the deformation characteristics of compacted particles. Hence, NIR spectroscopy could potentially serve as an alternative and complementary approach for exploring deformation characteristics and tablet density throughout the tablet compression process (Skelbæk-Pedersen et al., 2020). Peeters et al. have shown the advantages of using NIR and Raman spectroscopy complemented with traditional analysis methods (PSD, bulk and tapped density) can be effectively applied for a better understanding of granulation parameters that might affect tabletability (Peeters et al., 2016).

Recent advancements are not limited to real-time monitoring of various stages in the manufacturing process. They also emphasize the diverse characteristics of material behavior that can impact various compressibility indicators. Furthermore, there is a growing emphasis on employing multivariate analysis to address and understand batch-to-batch variations, particularly concerning issues like capping and lamination that can arise during the compression process (Mathe et al., 2023). Berkenkemper et al. have investigated material properties (PSD, Hausner factor, water content), tablet properties, tableting parameters and data from compression analysis. Principal component analysis (PCA) enabled the successful grouping of different materials based on these properties (Berkenkemper et al., 2023).

The complementarity of granule in-process control and different spectroscopic techniques in pharmaceutical manufacturing is a valuable approach that combines real-time monitoring of physical and chemical granule properties with advanced analytical techniques. This synergy provides a more comprehensive understanding of the manufacturing process, facilitates process optimization, and enhances and helps to maintain product quality.

The tableting properties of pharmaceutical products can be described through the compactibility and manufacturability parameters, as described by Osamura et al. (Osamura et al., 2016). Compactibility refers to the ability of a material to produce a mechanically strong tablet, being considered a critical quality attribute of this dosage form. Also, controlling stress values associated with tablet ejection is important during production, as an increased friction coefficient with the die wall can aggravate tablet failure and reduce manufacturability (Sun, 2015). Tablet failure can manifest as binding, capping, or lamination (Casian et al., 2019a; Djuris et al., 2019). Detachment stress is another valuable parameter for the control of the tableting process. The sticking tendency of the formulations can be detected by evaluating the detachment stress variations, as this parameter accounts for the friction between the lower punch and tablet during tablet detachment (Casian et al., 2019a).

This work proposed the development of a multi-instrumented PAT platform for the simultaneous prediction of granule downstream processability in terms of tabletability, detachment, and ejection stress. Predicting these attributes by fusing data derived from NIR spectra and particle size distributions is expected to provide better control of the tablet manufacturing process.

The novelty of this work stands in the development and evaluation of process analytical platforms that could accelerate the implementation of the QbC environment, with the ultimate objective of having continuously monitored and well-controlled processes that deliver consistent quality. Another relevant addition to the current state of knowledge is the use of data fusion strategies and artificial neural networks (ANN) based modeling for this purpose.

## 2. Materials and methods

### 2.1 Materials

Clopidogrel hydrogen sulphate, form II (MSN Laboratories Ltd, Telangana, India), Mannitol 35 (Pearlitol 50C) (Roquette Frères, Lestrem, France), Macrogol 8000 (Dow Chemical Company, Hahnville, LA, USA), Cellulose, microcrystalline M103D+ (Mingtai Chemical Co., Ltd., Taoyuan City, Taiwan), Low-substituted hydroxypropyl-cellulose (L-HPC, LH-11) (Shin-Etsu Chemical Co., Ltd., Tokyo, Japan). All the materials used in this study were of pharmaceutical grade.

### 2.2 Sample preparation

The calibration set formulations were prepared according to a full factorial experimental design (DoE) with three factors and two levels of variation. The granulation temperature, granulation time, and binder content were varied according to the matrix presented in Table 1. Factors were chosen based on a risk assessment approach. The identified critical process parameters (granulation temperature and time) were varied, taking into account the melting temperature of the binder, Macrogol 8000, as provided by the manufacturer (55 – 62°C), and literature data for granulation time, which falls within the range of 10 – 15 minutes (Kraciuk and Sznitowska, 2011). The testing limits for these critical process parameters were selected to encompass experiments inside and outside these specified intervals to capture as much variability in the process as possible. In completion, the binder content was varied based on literature data, which suggests using higher viscosity Macrogol types typically in the range of 10-15% w/w of the tablet weight for thermoplastic granulation (Rowe et al., 2009).

The active pharmaceutical ingredient (API) and selected excipients were granulated in a Bosch Solidlab 1 fluid-bed granulator and dryer (Bosch, Germany). The fluid-bed hot-melt granulation process consisted of three steps: 1. heating of the fluidized bed, 2. hot-melt granulation according to the predefined parameter setpoints in the experimental design, and 3. cooling. The qualitative and quantitative composition of the formulations are presented in Table 2.

**Table 1.** DoE matrix presenting factor variation during granule preparation

| Exp Name | Granulation time (min) | Temperature of fluidized bed (ºC) | Macrogol ( w/w %) |
|---|---|---|---|

| | | | |
|---|---|---|---|
| N1 | 5 | 50 | 8.109 |
| N2 | 30 | 50 | 8.109 |
| N3 | 5 | 65 | 8.109 |
| N4 | 30 | 65 | 8.109 |
| N5 | 5 | 50 | 13.886 |
| N6 | 30 | 50 | 13.886 |
| N7 | 5 | 65 | 13.886 |
| N8 | 30 | 65 | 13.886 |
| N9 | 5 | 50 | 18.244 |
| N10 | 30 | 50 | 18.244 |
| N11 | 5 | 65 | 18.244 |
| N12 | 30 | 65 | 18.244 |
| N13 | 17.5 | 57.5 | 13.886 |
| N14 | 17.5 | 57.5 | 13.886 |
| N15 | 17.5 | 57.5 | 13.886 |

N – formulation code

**Table 2.** Qualitative and quantitative ( w/w %) composition of formulations with different binder content included in the granulator

| Ingredients | N1 | N5 | N10 |
|---|---|---|---|
| Clopidogrel hydrogen sulphate | 39.996 | 39.996 | 39.996 |
| Mannitol | 31.056 | 28.178 | 25.988 |
| Macrogol 8000 | 8.109 | 13.886 | 18.244 |
| Cellulose, microcrystalline | 15.569 | 12.670 | 10.501 |
| Low-substituted hydroxypropyl-cellulose | 5.271 | 5.271 | 5.271 |

2.3 Sample selection for calibration and external validation

Each formulation was unloaded from the granulator, and for all the 15 factorial design points, 6 (S1-S6), 2-gram sized samples were taken in separate holders, resulting in a total of 90 granule samples. The samples were characterized using the proposed PAT tools and dynamic compaction analysis, ensuring an actual correspondence between process analytical data and tableting performance. Samples S2 and S5 from each formulation were used as external prediction sets (33.3%), whereas the other samples were used to train the models (66.6%).

2.4 NIR spectroscopy

Transmittance NIR spectra were recorded using an MPA NIR spectrometer (Bruker Optics, Germany) by selecting a rotating sample configuration. Each spectrum was recorded through OPUS 6.5 software using a resolution of 8 $cm^{-1}$ over the 12 497.2–6173.39 $cm^{-1}$ spectral range and by integrating 32 scans.

Reflectance NIR spectra were recorded through a fiber optic probe (Solvias Reflector HT2, USA) using an MPA NIR spectrometer (Bruker Optics, Germany). Spectra were recorded in the 11 550 – 3950 $cm^{-1}$ range with a resolution of 8 $cm^{-1}$ and through the accumulation of 16 scans. Each sample was characterized using both the transmittance and reflectance configurations, with 10 spectra per sample recorded by each method. That is, a total of 1800 spectra were recorded.

2.5 Particle Size Analysis

Particle size measurement of granule samples was done using a laser diffraction method with a Malvern Mastersizer 2000 (Malvern Instruments, Worcestershire, UK) equipped with a

Malvern Scirocco 2000 dry dispersion unit. The measurement was performed in dry dispersion mode, using approx. 1 g sample per measurement, with a measurement time of 6 s and using 1 bar dispersive air pressure. The Malvern Mastersizer 2000 uses the Mie scattering theory to calculate the particle size distribution, for which the particle refractive index and absorption value of 1.520 and 0.1 were assumed, respectively. These values provided weighted residuals of approx. 0.3% between the calculated data and the measurement, indicating a good value of the refractive index and absorption value. The obtained particle size distributions and the calculated d10, d50, d90, and span values were used for data analysis.

2.6 Dynamic compaction analysis

Dynamic compaction analysis was performed using a single punch Gamlen GTP, series D tablet Press (Gamlen Tableting Ltd., Biocity Nottingham, Nottingham, UK). 100 mg-sized tablets were compacted using 6 mm punches at a 10 mm/min speed over the 100 kg–200 kg–300 kg–400 kg–500 kg load range. The obtained force-displacement curves were used to calculate stress values during detachment (DS) and ejection (ES). Tensile strength (TS) was calculated using crushing force, diameter, and thickness (Eq.1).

$$\sigma = \frac{2 * F}{D * t * \pi}$$

F-crushing force (N); D-diameter; t-thickness Eq. 1

DS (MPa) was calculated as the ratio between the maximum detachment force and the compact surface area (Eq.2)

$$DS = \frac{F_d}{\pi * r^2}$$

$F_d$-maximum detachment force (N); r-compact radius Eq. 2

ES (MPa) was calculated as the peak ejection force divided by the compact diameter multiplied by the in-die thickness and constant π

$$ES = \frac{F_e}{\pi * D * t}$$

$F_e$- peak ejection force (N); D-diameter; t-thickness Eq. 3

The crushing force was measured using a hardness tester (Pharma-Test, Germany), while the compact diameter and thickness were measured using an electronic caliper (Yato tools, China).

2.7 Multivariate data analysis

2.7.1 Exploratory Data Analysis

Exploratory data analysis of NIR and PSD data was performed with PCA/OPLS to identify common and unique sources of variability. In this respect, the total variability in each data set was decomposed into predictive and orthogonal components and further investigated by generating pq column plots. The p and q loadings reflect the covariances between the

predictive score vector t and X variables and the covariances between the predictive score vector u and Y variables. The plot was used to identify variables that strongly contribute to the model and evaluate the relationship between X (NIR data) and Y (PSD data) variables.

### 2.7.2 PLS-based modeling

PLS models were developed considering individual and fused data sources to predict TS/ES/DS over the tested load range. The X variables were centered for individual data sources, whereas for fused data sources, the extracted latent variables were scaled to unit variance. The response variables were scaled to unit variance. The performance of calibration models was evaluated by considering the value of explained variability (R2), predictive capacity (Q2), the number of PLS factors, the root mean square error of cross-validation (RMSECV) and the root mean squared error of prediction (RMSEP). The optimal number of principal components was determined through 7-fold cross-validation and by comparing the prediction error sum of squares for different dimensions.

Mid-Level Data Fusion (MLDF) strategies were implemented by fusing features extracted from NIR and PSD. Feature extraction was performed by PCA through the calculation of latent variables. An optimal number of PCs was computed and considered for each data set based on the associated eigenvalue (>2). For PSD data, feature extraction was also tested by calculating the d10-d50-d90 parameters.

Considering input data structure, three types of fused models were developed. MLDF-1 models combined latent variables extracted from NIR and PSD data, MLDF-2 models combined NIR latent variables with d10-d50-d90 values from PSD and MLDF-3 type models also included process conditions and binder content with respect to MLDF-2. These models were developed by separately considering transmittance NIR and reflectance NIR spectra and their combination. The predictive ability of the models was tested on external samples. The influence of input data structure on the predictive performance of the models was evaluated more extensively on PLS-based models due to a more time-efficient model development compared to ANN. PLS-based data analysis was performed with SIMCA 17 (Sartorius Stedim, Sweden).

### 2.7.3 Artificial neural network based modeling

Artificial neural networks (ANNs) were built in MATLAB 9.12. (MathWorks, USA) using Statistics and Machine Learning Toolbox 12.3 and Deep Learning Toolbox 14.4. Feed-forward, fully-connected neural networks with one input, one hidden, and one output layers were developed to predict the TS/ES/DS. Different combinations of the following variables were tested as inputs: scores of the first two PCA variables obtained from the reflection and transmission NIR spectra, granulation process parameters, PSD data (scores of the first three OPLS variables or the d10-d50-span values), and the predicted macrogol concentration obtained by a PLS model. The output layer consisted of 5 neurons, corresponding to the TS/ES/ES values at the 5 different compaction loads. The optimal neuron number in the hidden layer was determined by systematically building ANNs with 1 – 10, 15, 20, and 30 neuron numbers with 50 repetitions at each number. The neuron number providing the lowest RMSE values for validation was used in the final model. Tangent sigmoid and linear transfer functions

were utilized in the hidden and the output neurons, respectively. The ANNs were trained by error backpropagation, using the Nguyen-Widrow layer initialization function for the initialization of the weights and biases, Bayesian regularization as the training algorithm, and the mean squared error (MSE) between the outputs and targets as the cost function. Due to the stochastic nature of the ANN training, bootstrap resampling was utilized with 200 sampling and, correspondingly 200 ANN model training for each model. In this way, the result of the ANN model refers to the average outcome of the 200 bootstrapped submodels, and the 95% confidence interval of the model prediction is estimated as the 2.5 and 97.5 percentiles of the 200 repetitions.

### 2.8 Prediction error analysis

The predictive performance was evaluated in relation to the independent variables considered for granule preparation (granulation temperature, granulation time, macrogol content) and the compaction load. The influence of these factors on the RMSEP values was investigated using a DoE approach by blocking the DoE matrix presented in Table 1 with the variation levels of the compaction load.

RMSEP variation was modeled using multiple linear regression (MLR), and the obtained models were evaluated considering the R2, Q2, Reproducibility, Validity parameters, and ANOVA-based model significance tests.

Thus, the robustness of predictions to these factors was easily evaluated through the significance of the models and the interpretation of the corresponding coefficient plots. The MLDF models were considered robust when the ANOVA test revealed a non-statistically significant difference between the modeled variation and the un-modeled variation of RMSEP ($p>0.05$), meaning that the prediction errors were not influenced by the factors varied during granule preparation and compaction.

## 3. Results and discussions

### 3.1 Tableting properties of the granulated formulations

The distribution of tableting properties within the applied load range revealed that with increasing compression load, the differences between formulations became more visible (the interquartile range became wider). Thus, the varied factors during granule manufacturing impacted their downstream processability, and discriminating between batches with good and poor tableting properties could be beneficial from a tableting throughput point of view. The properties of the granules are presented in Tables S1 and S2.

The effectiveness of the applied compression load in rising tablet hardness is represented in the tabletability plot (Fig 1a). The tabletability profile of the calibration set formulations revealed a linear increase, being controlled by the pressure-induced inter-particulate contact area. For some formulations, a plateau was reached for the TS after a linear increase, suggesting that a finite contact area was reached before the maximum applied load (Alderborn, 2003; Persson et al., 2022; Tye et al., 2005).

The detachment and ejection stress of the calibration set granules increased with increasing compaction load, indicating increasing friction at the tablet and die wall interface. At lower loads, the ejection stress presented a lower variation interval, and with increasing load,

the formulations became more differentiated (Fig 1b,c). The obtained variation domain was considered significant for an appropriate calibration.

Figure 1.

3.2 Development of regression models using individual PAT tools

Vibrational spectroscopic tools play a key role in implementing the PAT concept for monitoring critical quality and performance attributes of drug products. The analytical data recorded through these instruments contain multiple sources of variability, which could be related to the sample's chemical or physical properties, sample presentation, and environmental factors. Thus, pre-processing tools can come in handy by ensuring better control of undesired sources of variability.

The models developed for the prediction of tableting properties enabled the comparison of the selected instruments. Optimal models would combine a large R2X (predictive variability of input data), large Q2 (predictive performance), and low RMSECV/ RMSEP values. An increased predictive variability is desirable as it ensures an improved robustness of method performance.

In the case of tablet TS, the predictive variability found in raw transmittance NIR spectra was the largest out of the instruments (93%) and was negatively influenced by the use of spectral filters. Thus, applying pre-processing tools reduced the spectral variation correlated with granule tabletability. Applying the first derivative with a smoothing algorithm for reflectance NIR spectra increased the predictive variability, although the best predictive performance (lowest RMSEP) was also obtained from raw spectral data (Table S3).

Granule tabletability could also be predicted from particle size distribution data but with slightly larger RMSEP than NIR methods. As the surface area of the material that contributes to the formation of inter-particulate bonds is particle size dependent, model performance results suggest that the particle size distribution is also a good predictor.

The prediction of stress values associated with the ejection and detachment process worked better from particle size distribution type predictors, while the NIR tools presented a similar performance (Table 3). The higher complexity of PSD-based models could be attributed to the higher diversity of profile shapes and the independent variation of variable groups with respect to each other.

**Table 3.** Performance parameters of individual models fitted by PLS

| Instrument | Data | Spectral range ($cm^{-1}$) | PCs | R2X-pred | Q2 | RMSECV | RMSEP |
|---|---|---|---|---|---|---|---|
| Tensile strength | | | | | | | |
| NIR-t | raw spectra | 12493.3 – 6202.31 | 5 | 0.93 | 0.818 | 0.178 | 0.196 |

| | | | | | | | |
|---|---|---|---|---|---|---|---|
| NIR-r | raw spectra | 11544 – 3952 | 4 | 0.465 | 0.815 | 0.181 | 0.188 |
| Malvern | PSD | | 5 | 0.62 | 0.796 | 0.187 | 0.214 |
| Detachment stress | | | | | | | |
| NIR-t | raw spectra | 12493.3 – 6202.31 | 5 | 0.794 | 0.457 | 0.546 | 0.491 |
| NIR-r | raw spectra | 11544 – 3952 | 4 | 0.512 | 0.351 | 0.609 | 0.539 |
| Malvern | PSD | | 10 | 0.314 | 0.672 | 0.389 | 0.394 |
| Ejection stress | | | | | | | |
| NIR-t | raw spectra | 12493.3 – 6202.31 | 4 | 0.827 | 0.366 | 0.657 | 0.668 |
| NIR-r | raw spectra | 11544 – 3952 | 4 | 0.680 | 0.386 | 0.648 | 0.652 |
| Malvern | PSD | | 10 | 0.702 | 0.858 | 0.320 | 0.300 |

3.3 Evaluation of dataset complementarity

Using relevant input variables is essential for obtaining an optimal model performance. Therefore, the fusion of multiple data sources should be performed after applying a preliminary investigation of information complementarity. This procedure can justify using various feature extraction procedures and the optimal fusion strategy without relying only on a trial-and-error approach (Casian et al., 2022b).

The influence of independent variables on the recorded analytical data was evaluated by observing the clustering/ grouping of observations in score plots (Fig. 2) generated from models presented in section 3.2. In the case of transmittance NIR spectra, observations were clearly delimited with respect to the macrogol content variations and granulation temperature. The lower and upper levels of variation were clearly separated for granulation temperature, whereas the intermediate level was overlaid with the low temperature. The granulation time did not contribute to the systematic variability in the spectral data. Similar results were obtained for NIR reflectance data, although the cluster separation in the score plot is less clear (Fig. 2b.d).

The evaluation of experimental data revealed that the macrogol content and granulation temperature positively influenced the granules' growth during granulation (not shown). The PSD of the product influenced the TS, with larger granules offering an improved tabletability (Fig. 3c). Also, for the NIR instruments, the tabletability of the granules was well correlated with the baseline shift of the spectra (Fig.3a,b). Therefore, for the implementation of fusion strategies, raw NIR data was used for feature extraction.

Figure 2.

Figure 3.

OPLS models were developed to assess the complementarity between instruments, allowing the decomposition of the total variability into joint and unique sources (Table 4; Table S4). Thus, the NIR data was used as the X dataset, and PSD data was set as the Y dataset.

A similar correlation structure was identified with PSD for both transmittance and reflectance NIR spectra, implying two predictive components in the joint sources of variation. Approximately 70% of spectral variability (NIR-t: 69.7%; NIR-r: 74.3%) was correlated with 50% of particle size variation from the PSD profiles. The remaining part of data variability was summarised in orthogonal components. These results suggest that a large part of the information is overlapped, but each data source contains unique information that can bring additional value to the data fusion application. Although NIR data approximates well the PSD of the samples, the remaining fraction of orthogonal PSD variability is high and should be considered relevant.

**Table 4.** OPLS model results for complementarity evaluation

| NIR t vs PSD | | | |
|---|---|---|---|
| Component | Nr. of components | R2X (cum) | R2Y(cum) |
| Model | 2+5+3 | 0.99 | 0.998 |
| Predictive | 2 | 0.697 | 0.505 |
| Orthogonal-NIRt | 5 | 0.293 | |
| Orthogonal-PSD | 3 | | 0.493 |
| NIR r vs PSD | | | |
| Component | R2X | R2X (cum) | R2Y(cum) |
| Model | 2+2+2 | 0.999 | 0.993 |

| | | | |
|---|---|---|---|
| Predictive | 2 | 0.743 | 0.509 |
| Orthogonal-NIRr | 2 | 0.257 | |
| Orthogonal-PSD | 2 | | 0.484 |

The pq loadings of the OPLS models revealed that the NIR spectra capture the increase in particle size of the granules as a decrease in the baseline shift (negative p loadings) for transmittance data and as an increase (positive p loadings) for reflectance data (Fig. 4). These baseline shift variations were well correlated with a shift of particles from smaller size fractions towards larger ones.

Figure 4.

In the case of PSD data, the orthogonal variability relates to changes in particle size that were not captured well by spectral data. However, the orthogonal spectral variability can originate from various sources due to the multivariate nature of the NIR method. To further evaluate these effects, the decomposed spectral variability in the form of predictive and orthogonal latent variables was regressed against factors varied during granule preparation.

The generated loadings revealed that the predictive components (t1,t2) were well correlated with factors that influenced the particle size of the granules, namely the macrogol content and the granulation temperature (Fig. 5). Additionally, for both NIR methods, some of the orthogonal latent variables (to1-to5) contained information related to the composition of the granules. The correlation of these scores (to2-to5 for NIR-t; to1-to2 for NIR-r) with the samples' binder content confirmed this factor's unique contribution to the spectral variability. All the previously mentioned coefficients were significant, as the corresponding 95% confidence intervals suggested.

Although the binder content influenced particle growth during granulation, the extent of particle growth also depended on the granulation temperature and granulation time. Therefore, some formulations – despite the high content of Macrogol – did not granulate entirely due to the lower granulation temperature and time.

Figure 5.

By decomposing the total variability into common/joint and unique sources, it was highlighted that NIR data captured a significant part of particle size variation. However, both methods also contained relevant unique information. These sources were related to sample composition for NIR data and to particle size variations in the PSD profiles. Thus, a data fusion approach was justified for this application.

### 3.4 Data fusion strategies

The structure and the particularities of the datasets should drive the identification of an appropriate data fusion method. In this respect, MLDF is preferred when first-order data is

combined with a zero-order or another first-order dataset (Casian et al., 2022b). The available datasets in this study have a first-order structure, each sample being characterized by multiple variables. Moreover, considering the difference in the number of variables, an MLDF approach will ensure a more appropriate balance and avoid the domination of NIR over the PSD variables.

The faster computation of PLS compared to ANN models allowed the comparison of various input combinations, as presented in Figure 6.

Figure 6.

Based on the obtained performance parameters, the predictive ability of the models dropped in the following order: tensile strength, ejection stress, and detachment stress (Table 5).

**Table 5.** Performance parameters of MLDF models fitted by PLS method

| Y | Model name | MLDF Nr | NIR Instrument | PCs | R2X-pred | Q2 | RMSECV | RMSEP |
|---|---|---|---|---|---|---|---|---|
| TS | PLS-DF-M1 | 1 | NIR-t | 7 | 0.823 | 0.805 | 0.184 | 0.200 |
| | PLS-DF-M2 | 2 | NIR-t | 2 | 0.903 | 0.829 | 0.173 | 0.184 |
| | PLS-DF-M3 | 3 | NIR-t | 3 | 0.86 | 0.845 | 0.163 | 0.181 |
| | PLS-DF-M4 | 1 | NIR-r | 3 | 0.773 | 0.763 | 0.202 | 0.205 |
| | PLS-DF-M5 | 2 | NIR-r | 2 | 0.843 | 0.824 | 0.174 | 0.184 |
| | PLS-DF-M6 | 3 | NIR-r | 3 | 0.819 | 0.844 | 0.165 | 0.181 |
| | PLS-DF-M7 | 1 | NIR-t&NIR-r | 5 | 0.732 | 0.826 | 0.174 | 0.188 |
| | PLS-DF-M8 | 2 | NIR-t&NIR-r | 2 | 0.802 | 0.834 | 0.170 | 0.183 |

| | | | | | | | | |
|---|---|---|---|---|---|---|---|---|
| | PLS-DF-M9 | 3 | NIR-t&NIR-r | 3 | 0.793 | 0.849 | 0.161 | 0.180 |
| ES | PLS-DF-M10 | 1 | NIR-t | 4 | 0.658 | 0.642 | 0.451 | 0.446 |
| | PLS-DF-M11 | 2 | NIR-t | 6 | 0.676 | 0.531 | 0.571 | 0.554 |
| | PLS-DF-M12 | 3 | NIR-t | 6 | 0.652 | 0.535 | 0.552 | 0.555 |
| | PLS-DF-M13 | 1 | NIR-r | 4 | 0.665 | 0.701 | 0.414 | 0.395 |
| | PLS-DF-M14 | 2 | NIR-r | 3 | 0.862 | 0.435 | 0.613 | 0.599 |
| | PLS-DF-M15 | 3 | NIR-r | 8 | 0.66 | 0.546 | 0.548 | 0.557 |
| | PLS-DF-M16 | 1 | NIR-t&NIR-r | 5 | 0.594 | 0.701 | 0.422 | 0.413 |
| | PLS-DF-M17 | 2 | NIR-t&NIR-r | 5 | 0.681 | 0.492 | 0.585 | 0.573 |
| | PLS-DF-M18 | 3 | NIR-t&NIR-r | 7 | 0.611 | 0.546 | 0.555 | 0.558 |
| DS | PLS-DF-M19 | 1 | NIR-t | 3 | 0.889 | 0.486 | 0.546 | 0.493 |
| | PLS-DF-M20 | 2 | NIR-t | 6 | 0.859 | 0.533 | 0.508 | 0.450 |
| | PLS-DF-M21 | 3 | NIR-t | 4 | 0.909 | 0.484 | 0.516 | 0.457 |

| | | | | | | | |
|---|---|---|---|---|---|---|---|
| PLS-DF-M22 | 1 | NIR-r | 4 | 0.689 | 0.486 | 0.548 | 0.505 |
| PLS-DF-M23 | 2 | NIR-r | 6 | 0.795 | 0.518 | 0.520 | 0.454 |
| PLS-DF-M24 | 3 | NIR-r | 9 | 0.597 | 0.57 | 0.469 | 0.430 |
| PLS-DF-M25 | 1 | NIR-t&NIR-r | 4 | 0.683 | 0.51 | 0.516 | 0.476 |
| PLS-DF-M26 | 2 | NIR-t&NIR-r | 4 | 0.871 | 0.448 | 0.545 | 0.491 |
| PLS-DF-M27 | 3 | NIR-t&NIR-r | 5 | 0.806 | 0.498 | 0.503 | 0.449 |

During the application of MLDF, the feature extraction procedure should efficiently capture the data structure and avoid the loss of predictive information. Comparing the effect of feature extraction and the selected input variables, the use of d10-50-90 parameters was more beneficial than PCA scores of the PSD, and the addition of process data had only a slight positive effect on the prediction of TS and DS. In the case of ES, PCA scores calculated from PSD data worked better, and the addition of process data was redundant and slightly increased the prediction errors. Using PLS-based modeling, the prediction errors of the investigated responses were comparable to the individual methods.

Comparing the prediction errors between models using as input d10-50-90 or PCA scores of full PSD highlighted that predictions for some samples with a non-ideal distribution were superior to latent variable type predictors. However, these bi-modal or skewed-shaped PSD profiles were also present in samples where the d10-50-90 type feature extraction was similar or performed better than the calculation of latent variables. Based on the experimental results, the criteria for selecting the feature extraction method for PSD data can not be defined based on the shape of the distribution.

ANN modeling was also evaluated as a data fusion method, providing different combinations of the PAT measurements as model inputs. The results of the build models are summarized in Table 6. For TS, ES, and DS, a model (M1) was built with all the possible input variables (i.e., NIR-r, NIR-t, d10-d50-d90, PSD scores, granulation parameters, and predicted macrogol concentration), as well as using only the NIR-t, NIR-r data (M2). Furthermore, some more random combinations of the inputs were also tested (M3-M6/4). Comparing the $R^2$ and RMSE values of the PLS and ANN models, it was observed that the ANNs systematically provided superior model performance; for example, the best TS, ES, and DS prediction with

ANN resulted in an RMSEP of 0.119, 0.256, and 0.293 as opposed to the 0.180, 0.395 and 0.430 RMSEPs of the PLS models, respectively. The impact of different input combinations on the ANNs performance could also be analyzed. The ANNs resulted in the highest errors for all response variables when only the NIR spectra (i.e., their PCA scores) were provided as inputs. Including the PSD of the granules (either as a PCA score or as the d10-d50-d90-span values) was found to be essential to improve the model accuracy, which corresponds to the results of the OPLS, i.e., that the NIR approximates well the PSD of the samples. However, the remaining fraction of the orthogonal PSD variability is also relevant. Apart from this, the different combinations of inputs, including all the possible features in the model, resulted in only marginal differences. This indicates that the ANN could successfully assess the importance of the inputs during the training process, and therefore, ANNs can be a powerful tool for data fusion. A possible reason for the superior performance of the ANN data fusion method compared to the PLS approach is that ANN can account for the potential non-linear relationships in the datasets.

Furthermore, ANNs can efficiently select relevant information by appropriately weighting the inputs during training. Although PLS modeling also aims to retain only the most substantial information during the projection to latent variables, this process still considers all the original variables. This could improve the model's results if an appropriate variable selection method is used.

**Table 6.** Performance parameters of MLDF models fitted by ANN method

| Response | DF | Input | Neuron number | R2 (train) | R2 (test) | RMSEC | RMSEP |
|---|---|---|---|---|---|---|---|
| TS | ANN-TS-M1 | All data | 7 | 0.971 | 0.922 | 0.075 | 0.123 |
| | ANN-TS-M2 | NIR-r, NIR-t | 7 | 0.914 | 0.864 | 0.125 | 0.159 |
| | ANN-TS-M3 | d10-d50-d90-span, Process conditions, Pred. macrogol | 8 | 0.962 | 0.918 | 0.086 | 0.127 |
| | ANN-TS-M4 | NIR-r, NIR-t, d10-d50-d90-span, Process conditions, Pred. macrogol | 8 | 0.972 | 0.925 | 0.074 | 0.121 |

| | | | | | | | |
|---|---|---|---|---|---|---|---|
| | ANN-TS-M5 | NIR-r, NIR-t, d10-d50-d90-span, Process conditions | 8 | 0.968 | 0.926 | 0.078 | 0.119 |
| | ANN-TS-M6 | NIR-r, NIR-t, PSD scores, Process conditions | 8 | 0.968 | 0.924 | 0.079 | 0.121 |
| ES | ANN-ES-M1 | All data | 6 | 0.921 | 0.897 | 0.199 | 0.259 |
| | ANN-ES-M2 | NIR-r, NIR-t | 6 | 0.600 | 0.527 | 0.363 | 0.406 |
| | ANN-ES-M3 | d10-d50-d90-span, Process conditions, PSD scores, Pred. macrogol | 7 | 0.913 | 0.901 | 0.218 | 0.256 |
| | ANN-ES-M4 | NIR-r, NIR-t, PSD scores | 8 | 0.917 | 0.898 | 0.205 | 0.261 |
| DS | ANN-DS-M1 | All data | 3 | 0.709 | 0.683 | 0.250 | 0.307 |
| | ANN-DS-M2 | NIR-r, NIR-t | 1 | 0.421 | 0.437 | 0.369 | 0.337 |
| | ANN-DS-M3 | Process conditions, d10-d50-d90-span, PSD scores, Pred. macrogol | 3 | 0.706 | 0.684 | 0.253 | 0.307 |
| | ANN-DS-M4 | NIR-r, d10-d50-d90-span, Process conditions, Pred. macrogol | 3 | 0.685 | 0.690 | 0.251 | 0.293 |

* All data: NIR-r, NIR-t, d10-d50-d90-span, PSD scores, Process conditions, Pred. macrogol

Figure 7.

3.5 Prediction error analysis

Reaching a robust model performance would assume an independent variation of prediction errors with respect to the factors varied during granule preparation and compression, meaning that the accuracy of predictions is similar within the entire experimental region/ calibration space. To this respect, an RMSEP value was computed separately for each formulation and introduced in the worksheet of the DoE matrix.

3.5.1 Tensile strength

The distribution of RMSEP values for TS was similar for the individual instruments and PLS-based DF models, with a slightly wider interquartile range for PSD-type predictors (Fig. 8a). In this case, the variation of prediction errors was linked to the applied compression load (Fig. 9). Considering the increase of response variation with increasing load, depicted in figure 1, this is an expected outcome. The coefficient corresponding to the compression force was statistically significant for all the PLS-based models, with some differences in the size of the effect (Fig 9). The structure of the input data for PLS-based DF models did not significantly affect the prediction robustness.

Figure 8.

According to the ANOVA results for model significance, all ANN-based DF models presented a $p>0.05$ (M1-0.890; M2-0.861; M3-0.774; M4-0.929; M5-0.903; M6-0.133) and offered robust predictions independent of the input factor combination. Moreover, the coefficient plots of these models showed a non-significant effect from the compression load on the size of RMSEP values (Fig.9).

Figure 9.

3.5.2 Ejection and detachment stress

In the case of the stress parameters, the RMSEP distribution was better for models relying on PSD as predictors (Fig.8, b,c). An increase of compression load from 100 kg to 500 kg, while having all the other factors at an intermediate level, produced an increase of RMSEP value for ES/DS between 0.25-0.35 MPa for NIR-based models and only 0.15 MPa for PSD-based models ( Figures S1 and S2). Thus, predictions were more robust from PSD due to the lower impact of compression force variation.

For ES, the MLDF1 method (M10-M13-M16), relying on the use of PCA for feature extraction of NIR and PSD data, presented a smaller interquartile range compared to MLDF2 and 3 approaches (Fig.8b). In the case of DS, the distribution of RMSEP values for MLDF models fitted by PLS revealed no significant differences with respect to the feature extraction method and the structure of the input data (Fig.8c).

For these tableting parameters, the ANOVA values for model significance revealed that the input settings are linked to the predictive performance of these models, mainly through the significant effect of compression load. However, the magnitude of the effect was the smallest

for ANN-based models. Thus, selecting a modeling approach was important to ensure lower prediction errors in the calibration space.

Overall, the magnitude of prediction errors was reduced, having an average RMSEP±SD across all models of 0.158±0.110 MPa for TS, 0.400±0.284 MPa for DS, and 0.426±0.330 MPa for ES. Considering that for optimal tableting properties, the TS should be above 2MPa, and the stress values during detachment/ejection should be below 5MPa, the developed tool can be efficiently applied for improved control of the tableting process. Despite the off-line development, the PAT tool can already be used for the at-line prediction of tableting properties and the discrimination of batches with optimal and poor downstream processability. Knowing the tableting properties of the upstream materials will enable the operator to adjust the tableting speed, pre-compression force, compression force, and dwell time to ensure the preparation of tablets with reproducible quality.

## 4. Conclusions

This work proposed the development of a PAT platform for the simultaneous prediction of granule downstream processability by fusing transmittance NIR, reflectance NIR spectra, and particle size distribution type data.

Comparing the systematic variability in the two data types, it was highlighted that approximately 70% of spectral variability was correlated with 50% of particle size variation from the PSD profiles. Despite the large information overlap, each data source contained unique and relevant information for the fusion application. Using the OPLS method for variability decomposition confirmed that the unique spectral features were linked to compositional differences, mainly related to the varied binder content.

These particularities of the data sources could explain the differences in the performance of individual models. Granule tabletability was more accurately predicted from spectral data, meaning that the unique features in the NIR data presented a larger contribution. Although the binder content influenced particle growth during granulation, the extent of particle growth also depended on the granulation temperature and granulation time. Therefore, some formulations did not granulate completely despite the high binder content due to the lower granulation temperature and time. In such cases, the binder content of the formulation, relevant for granule tabletability, was more reliably captured by the NIR data compared to PSD. Stress values associated with tablet ejection and detachment were predicted more efficiently from PSD data. Thus, the more accurate description of particle size differences through PSD profiles (50% unique variability) proved relevant for estimating the product's manufacturability.

The faster PLS-based model development allowed the comparison of various input combinations and feature extraction methods for the MLDF models. The structure of the input data for PLS-based DF models did not significantly affect the predictive performance, as the RMSEP values were similar. Comparing PLS and ANN models, it was observed that the ANNs systematically provided superior model performance. For example, the best TS, ES, and DS prediction with ANN resulted in an RMSEP of 0.119, 0.256, and 0.293 as opposed to the PLS models' 0.180, 0.395, and 0.430 RMSEPs, respectively. For all response variables, the ANNs provided the highest errors when only features extracted from NIR data were used as predictors. In contrast, including features extracted from PSD profiles was important for increasing the predictive power.

Finally, the robustness of the developed models was assessed by evaluating the dependence of RMSEP values on the factors that varied during granule preparation and compression. For granule tabletability, all ANN-based models offered robust predictions, as the RMSEP values varied independently from the input factors. In the case of the individual and PLS-based MLDF models, the size of prediction errors depended on the applied compression load. In the case of the stress values, the RMSEP was influenced by the applied compression load, with a lower effect for ANN-based models. Thus, selecting a modeling approach was important to ensure lower prediction errors in the calibration space.

The results of this work demonstrate the advantages of fusing complementary sources of data for the control of complex quality attributes relevant to the tableting process.

Acknowledgments: This work was supported by a grant of the Ministry of Research, Innovation and Digitization, CNCS—UEFISCDI, project number PN-III-P1-1.1-PD-2021-0420, within PNCDI III.

**Tibor Casian:** Conceptualization, Data curation, Formal analysis, Methodology, Writing -

original draft **Brigitta Nagy:** Data curation, Formal analysis, Software, Writing - review & editing **Cristiana Lazurca:** Investigation **Victor Marcu:** Investigation **Erzsébet Orsolya Tőkés:** Investigation **Éva Katalin Kelemen:** Resources **Katalin Zöldi:** Resources **Radu Oprean:** Supervision, Validation **Zsombor Nagy:** Supervision **Ioan Tomuta:** Supervision **Béla Kovács:** Supervision, Methodology, Conceptualization, Writing - review & editing

References

Alam, M.A., Shi, Z., Drennen, J.K., Anderson, C.A., 2017. In-line monitoring and optimization of powder flow in a simulated continuous process using transmission near infrared spectroscopy. Int. J. Pharm. 526, 199–208. https://doi.org/10.1016/j.ijpharm.2017.04.054

Alderborn, G., 2003. A Novel Approach to Derive a Compression Parameter Indicating Effective Particle Deformability. Pharm. Dev. Technol. 8, 367–377. https://doi.org/10.1081/PDT-120024690

Berkenkemper, S., Klinken, S., Kleinebudde, P., 2023. Multivariate data analysis to evaluate commonly used compression descriptors. Int. J. Pharm. 637, 122890. https://doi.org/10.1016/j.ijpharm.2023.122890

Blanco, D., Antikainen, O., Räikkönen, H., Yliruusi, J., Juppo, A.M., 2021. Effect of colloidal silicon dioxide and moisture on powder flow properties: Predicting in-process performance using image-based analysis. Int. J. Pharm. 597, 120344. https://doi.org/10.1016/j.ijpharm.2021.120344

Casian, T., Borbás, E., Ilyés, K., Démuth, B., Farkas, A., Rapi, Z., Bogdan, C., Iurian, S., Toma, V., Știufiuc, R., Farkas, B., Balogh, A., Marosi, G., Tomuță, I., Nagy, Z.K.,

2019a. Electrospun amorphous solid dispersions of meloxicam: Influence of polymer type and downstream processing to orodispersible dosage forms. Int. J. Pharm. 569, 118593. https://doi.org/10.1016/j.ijpharm.2019.118593

Casian, T., Farkas, A., Ilyés, K., Démuth, B., Borbás, E., Madarász, L., Rapi, Z., Farkas, B., Balogh, A., Domokos, A., Marosi, G., Tomută, I., Nagy, Z.K., 2019b. Data fusion strategies for performance improvement of a Process Analytical Technology platform consisting of four instruments: An electrospinning case study. Int. J. Pharm. 567, 118473. https://doi.org/10.1016/j.ijpharm.2019.118473

Casian, T., Iurian, S., Gâvan, A., Porfire, A., Pop, A.L., Crișan, S., Pușcaș, A.M., Tomuță, I., 2022a. In-Depth Understanding of Granule Compression Behavior under Variable Raw Material and Processing Conditions. Pharmaceutics 14, 177. https://doi.org/10.3390/pharmaceutics14010177

Casian, T., Nagy, B., Kovács, B., Galata, D.L., Hirsch, E., Farkas, A., 2022b. Challenges and Opportunities of Implementing Data Fusion in Process Analytical Technology—A Review. Molecules 27, 4846. https://doi.org/10.3390/molecules27154846

De Bisshop, J., Klinken, S., 2023. Prediction of the tensile strength of tablets using LSTM networks on compression profiles. Int. J. Pharm. 645, 123280. https://doi.org/10.1016/j.ijpharm.2023.123280

Djuris, J., Milovanovic, S., Medarevic, D., Dobricic, V., Dapčević, A., Ibric, S., 2019. Selection of the suitable polymer for supercritical fluid assisted preparation of carvedilol solid dispersions. Int. J. Pharm. 554, 190–200. https://doi.org/10.1016/j.ijpharm.2018.11.015

Domokos, A., Pusztai, É., Madarász, L., Nagy, B., Gyürkés, M., Farkas, A., Fülöp, G., Casian, T., Szilágyi, B., Nagy, Z.K., 2021. Combination of PAT and mechanistic modeling tools in a fully continuous powder to granule line: Rapid and deep process understanding. Powder Technol. 388, 70–81. https://doi.org/10.1016/j.powtec.2021.04.059

Gavan, A., Iurian, S., Casian, T., Porfire, A., Porav, S., Voina, I., Oprea, A., Tomuta, I., 2020. Fluidised bed granulation of two APIs: QbD approach and development of a NIR in-line monitoring method. Asian J. Pharm. Sci. 15, 506–517. https://doi.org/10.1016/j.ajps.2019.03.003

Hattori, Y., Naganuma, M., Otsuka, M., 2020. Partial Least Squares Regression-Based Robust Forward Control of the Tableting Process. Pharmaceutics 12, 85. https://doi.org/10.3390/pharmaceutics12010085

Jelsch, M., Roggo, Y., Kleinebudde, P., Krumme, M., 2021. Model predictive control in pharmaceutical continuous manufacturing: A review from a user's perspective. Eur. J. Pharm. Biopharm. 159, 137–142. https://doi.org/10.1016/j.ejpb.2021.01.003

Jin, C., Zhao, L., Feng, Y., Hong, Y., Shen, L., Lin, X., 2022. Simultaneous modeling prediction of three key quality attributes of tablets by powder physical properties. Int. J. Pharm. 628, 122344. https://doi.org/10.1016/j.ijpharm.2022.122344

Kalies, A., Heinrich, T., Leopold, C.S., 2020. A novel approach to avoid capping and/or

lamination by application of external lower punch vibration. Int. J. Pharm. 580, 119195. https://doi.org/10.1016/j.ijpharm.2020.119195

Kraciuk, R., Sznitowska, M., 2011. Effect of Different Excipients on the Physical Characteristics of Granules and Tablets with Carbamazepine Prepared with Polyethylene Glycol 6000 by Fluidized Hot-Melt Granulation (FHMG). AAPS PharmSciTech 12, 1241–1247. https://doi.org/10.1208/s12249-011-9698-7

Madarász, L., Köte, Á., Gyürkés, M., Farkas, A., Hambalkó, B., Pataki, H., Fülöp, G., Marosi, G., Lengyel, L., Casian, T., Csorba, K., Nagy, Z.K., 2020. Videometric mass flow control: A new method for real-time measurement and feed-back control of powder micro-feeding based on image analysis. Int. J. Pharm. 580, 119223. https://doi.org/10.1016/j.ijpharm.2020.119223

Madarász, L., Köte, Á., Hambalkó, B., Csorba, K., Kovács, V., Lengyel, L., Marosi, G., Farkas, A., Nagy, Z.K., Domokos, A., 2022. In-line particle size measurement based on image analysis in a fully continuous granule manufacturing line for rapid process understanding and development. Int. J. Pharm. 612, 121280. https://doi.org/10.1016/j.ijpharm.2021.121280

Mathe, R., Casian, T., Tomuţă, I., 2020. Multivariate feed forward process control and optimization of an industrial, granulation based tablet manufacturing line using historical data. Int. J. Pharm. 591, 119988. https://doi.org/10.1016/j.ijpharm.2020.119988

Mathe, R., Casian, T., Marina, A., Marusca, D., Tomuta, I., 2023. Multivariate Data Analysis For Tableting Performance Improvement At Industrial Scale. A Case Study Focused On Understanding And Avoiding The Occurrence Of Capping And Lamination. Farmacia 71, 798–809. https://doi.org/10.31925/farmacia.2023.4.16

Mazel, V., Busignies, V., Diarra, H., Tchoreloff, P., 2015. Lamination of pharmaceutical tablets due to air entrapment: Direct visualization and influence of the compact thickness. Int. J. Pharm. 478, 702–704. https://doi.org/10.1016/j.ijpharm.2014.12.023

Mazel, V., Desbois, L., Tchoreloff, P., 2019. Influence of the unloading conditions on capping and lamination: Study on a compaction simulator. Int. J. Pharm. 567, 118468. https://doi.org/10.1016/j.ijpharm.2019.118468

Mazel, V., Tchoreloff, P., 2022. Lamination of Pharmaceutical Tablets: Classification and Influence of Process Parameters. J. Pharm. Sci. 111, 1480–1485. https://doi.org/10.1016/j.xphs.2021.10.025

Osamura, T., Takeuchi, Y., Onodera, R., Kitamura, M., Takahashi, Y., Tahara, K., Takeuchi, H., 2016. Characterization of tableting properties measured with a multi-functional compaction instrument for several pharmaceutical excipients and actual tablet formulations. Int. J. Pharm. 510, 195–202. https://doi.org/10.1016/j.ijpharm.2016.05.024

Paul, S., Sun, C.C., 2017. Gaining insight into tablet capping tendency from compaction simulation. Int. J. Pharm. 524, 111–120. https://doi.org/10.1016/j.ijpharm.2017.03.073

Pauli, V., Roggo, Y., Kleinebudde, P., Krumme, M., 2019. Real-time monitoring of particle size distribution in a continuous granulation and drying process by near infrared spectroscopy. Eur. J. Pharm. Biopharm. 141, 90–99.

https://doi.org/10.1016/j.ejpb.2019.05.007

Peeters, E., Tavares da Silva, A.F., Toiviainen, M., Van Renterghem, J., Vercruysse, J., Juuti, M., Lopes, J.A., De Beer, T., Vervaet, C., Remon, J.-P., 2016. Assessment and prediction of tablet properties using transmission and backscattering Raman spectroscopy and transmission NIR spectroscopy. Asian J. Pharm. Sci. 11, 547–558. https://doi.org/10.1016/j.ajps.2016.04.004

Persson, A.-S., Pazesh, S., Alderborn, G., 2022. Tabletability and compactibility of α -lactose monohydrate powders of different particle size. I. Experimental comparison. Pharm. Dev. Technol. 27, 319–330. https://doi.org/10.1080/10837450.2022.2051550

Porfire, A., Rus, L., Vonica, A.L., Tomuta, I., 2012. High-throughput NIR-chemometric methods for determination of drug content and pharmaceutical properties of indapamide powder blends for tabletting. J. Pharm. Biomed. Anal. 70, 301–309. https://doi.org/10.1016/j.jpba.2012.07.026

Rowe, R., Sheskey, P., Quinn, M., 2009. Handbook of Pharmaceutical Excipients, 6th ed, Pharmaceutical Press. Chicago. https://doi.org/10.1016/S0168-3659(01)00243-7

Saddik, J.S., Dave, R.H., 2021. Evaluation of powder rheology as a potential tool to predict tablet sticking. Powder Technol. 386, 298–306. https://doi.org/10.1016/j.powtec.2021.03.062

Skelbæk-Pedersen, A.L., Vilhelmsen, T.K., Wallaert, V., Rantanen, J., 2020. Investigation of the effects of particle size on fragmentation during tableting. Int. J. Pharm. 576, 118985. https://doi.org/10.1016/j.ijpharm.2019.118985

Sun, C.C., 2015. Dependence of ejection force on tableting speed—A compaction simulation study. Powder Technol. 279, 123–126. https://doi.org/10.1016/j.powtec.2015.04.004

Tye, C.K., Sun, C. (Calvin), Amidon, G.E., 2005. Evaluation of the effects of tableting speed on the relationships between compaction pressure, tablet tensile strength, and tablet solid fraction. J. Pharm. Sci. 94, 465–472. https://doi.org/10.1002/jps.20262

Wünsch, I., Finke, J.H., John, E., Juhnke, M., Kwade, A., 2021. The influence of particle size on the application of compression and compaction models for tableting. Int. J. Pharm. 599, 120424. https://doi.org/10.1016/j.ijpharm.2021.120424

Záhonyi, P., Fekete, D., Szabó, E., Madarász, L., Fazekas, Á., Haraszti, A., Nagy, Z.K., 2023. Integrated continuous melt granulation-based powder-to-tablet line: Process investigation and scale-up on the same equipment. Eur. J. Pharm. Biopharm. 189, 165–173. https://doi.org/10.1016/j.ejpb.2023.06.005

**Fig. 1** Distribution of TS (a), ES (b) and DS (c) values of calibration set samples in the load range of 100 – 500 kg

**Fig. 2** Score scatter plots revealing the grouping of spectral data for NIR t (left) and NIR r (right)

**Fig. 3** Raw NIR-t, NIR-r and PSD data colour coded according to tablet TS

**Fig. 4** Pq column plot of OPLS models developed for exploratory analysis purposes between NIR t and PSD (a), respectively NIR r and PSD (b).

**Fig. 5** The correlation between predictive/orthogonal components of spectral variability and factors varied during granule manufacturing. a)NIR-t, Macrogol %; b) NIR-t, granulation temperature; c) NIR-r, Macrogol %; d) NIR-r, granulation temperature;

t1,t2 – predictive components capturing spectral variability correlated with changes in PSD;

to1-to5 – orthogonal components capturing spectral variability not correlated with changes in PSD;

**Fig. 6** MLDF options considered for the prediction of granule tableting properties

**Fig. 7** Tabletability (a), ejection (b) and detachment stress (c) profiles predicted by PLS and ANN methods

**Fig. 8** Distribution of RMSEP values for individual and DF models built to predict TS (a), ES (b), DS (c)

**Fig. 9** Coefficient loading plots revealing the influence of factors varied during granule preparation on the RMSEP values for TS

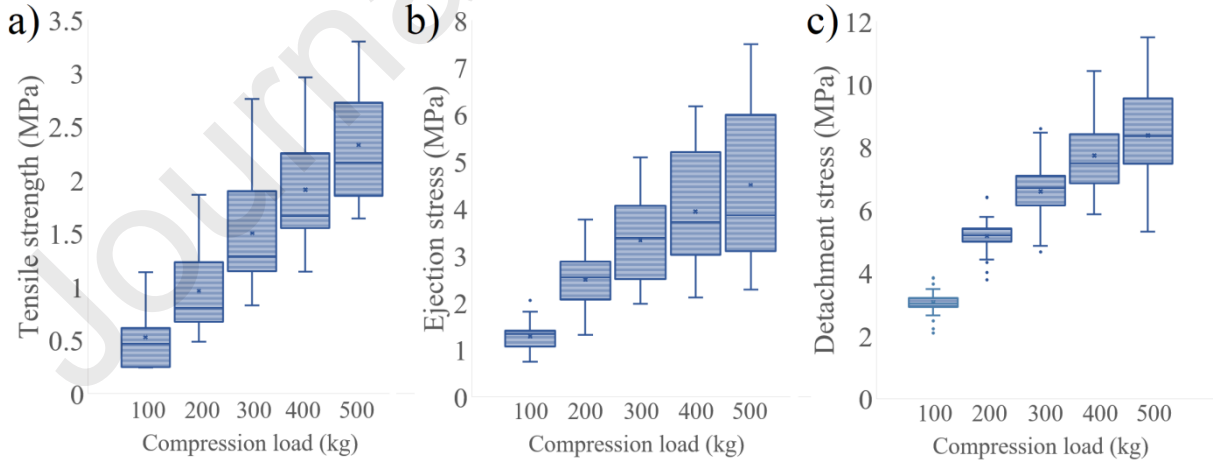


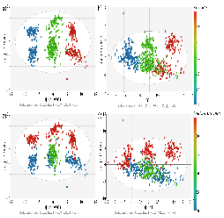

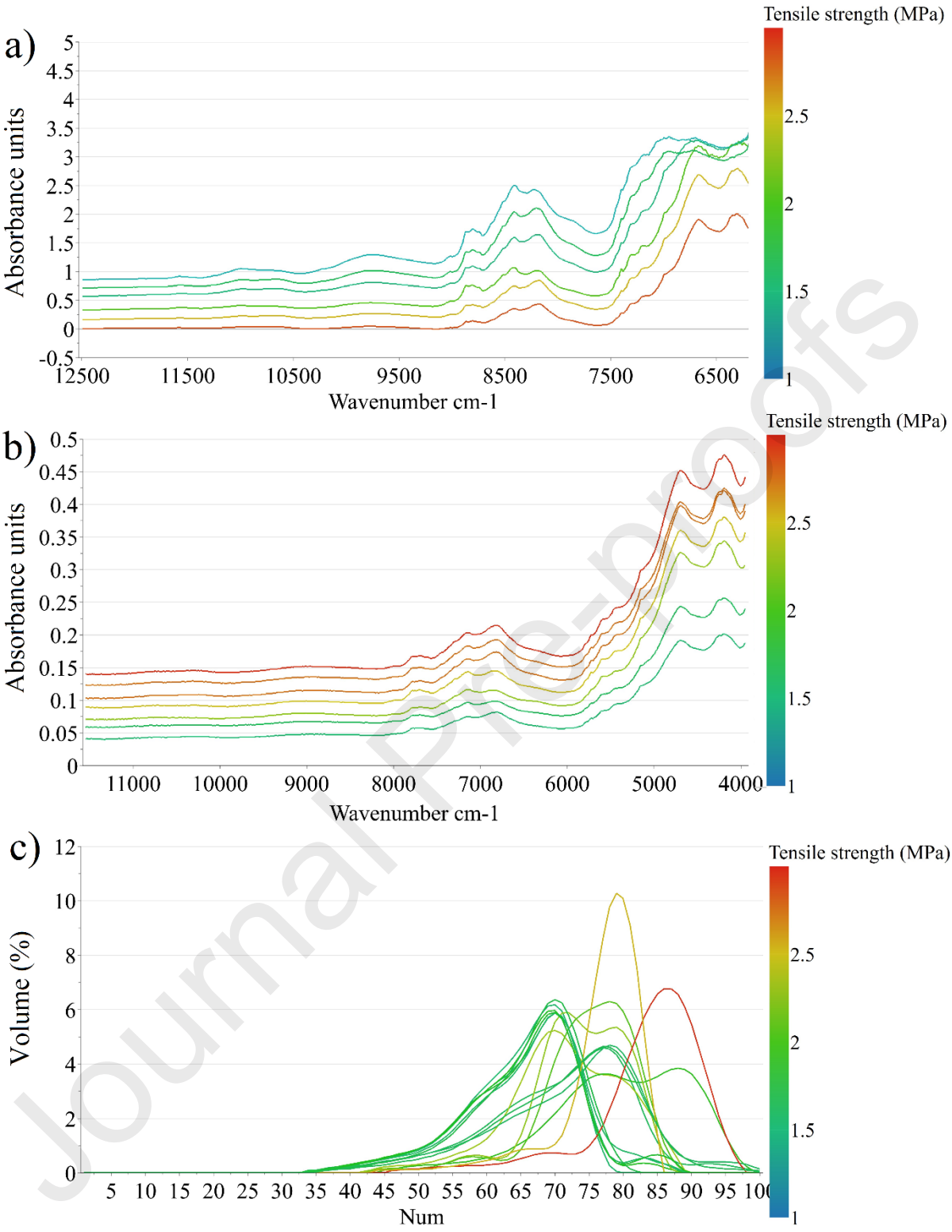

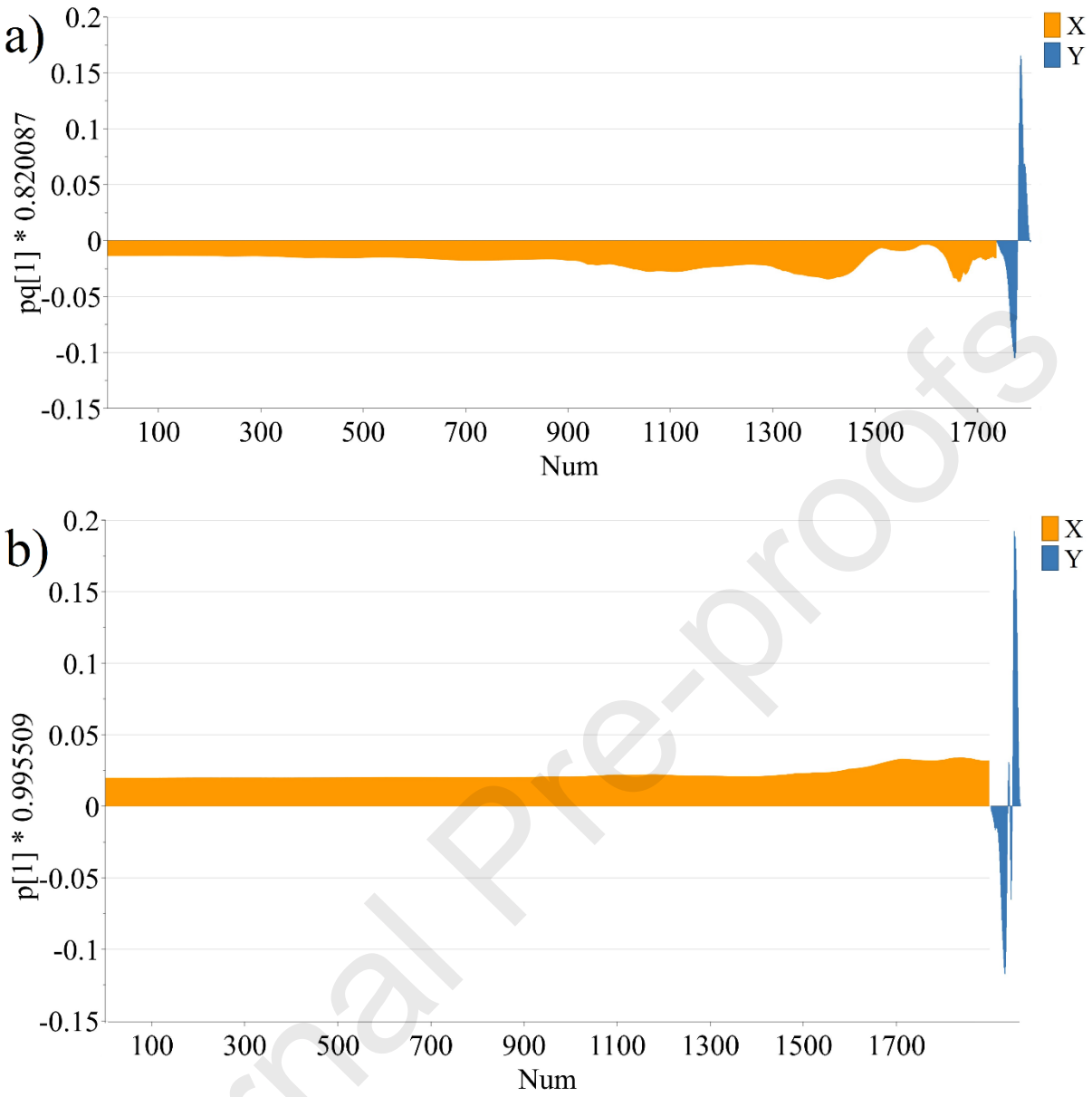

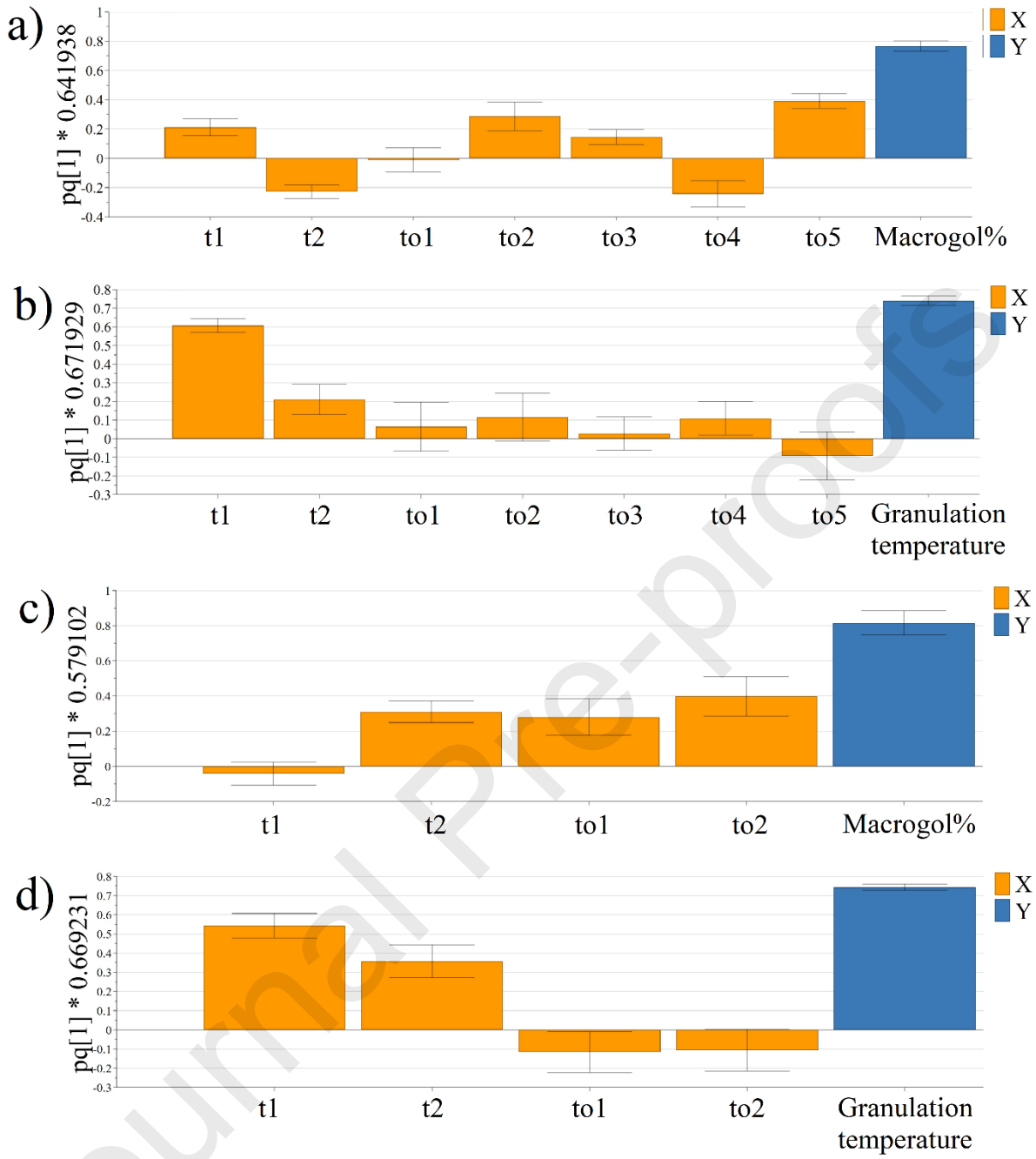

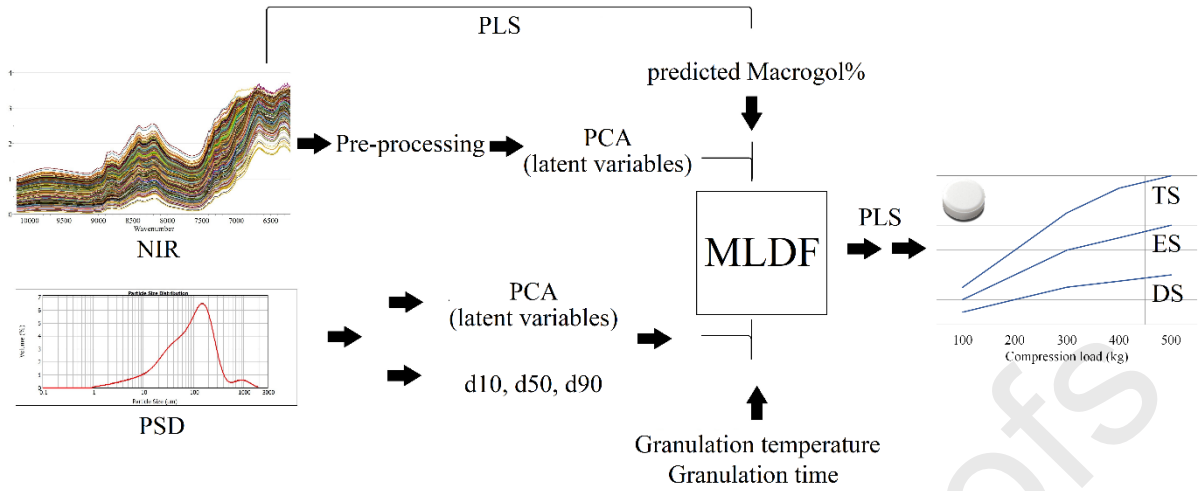

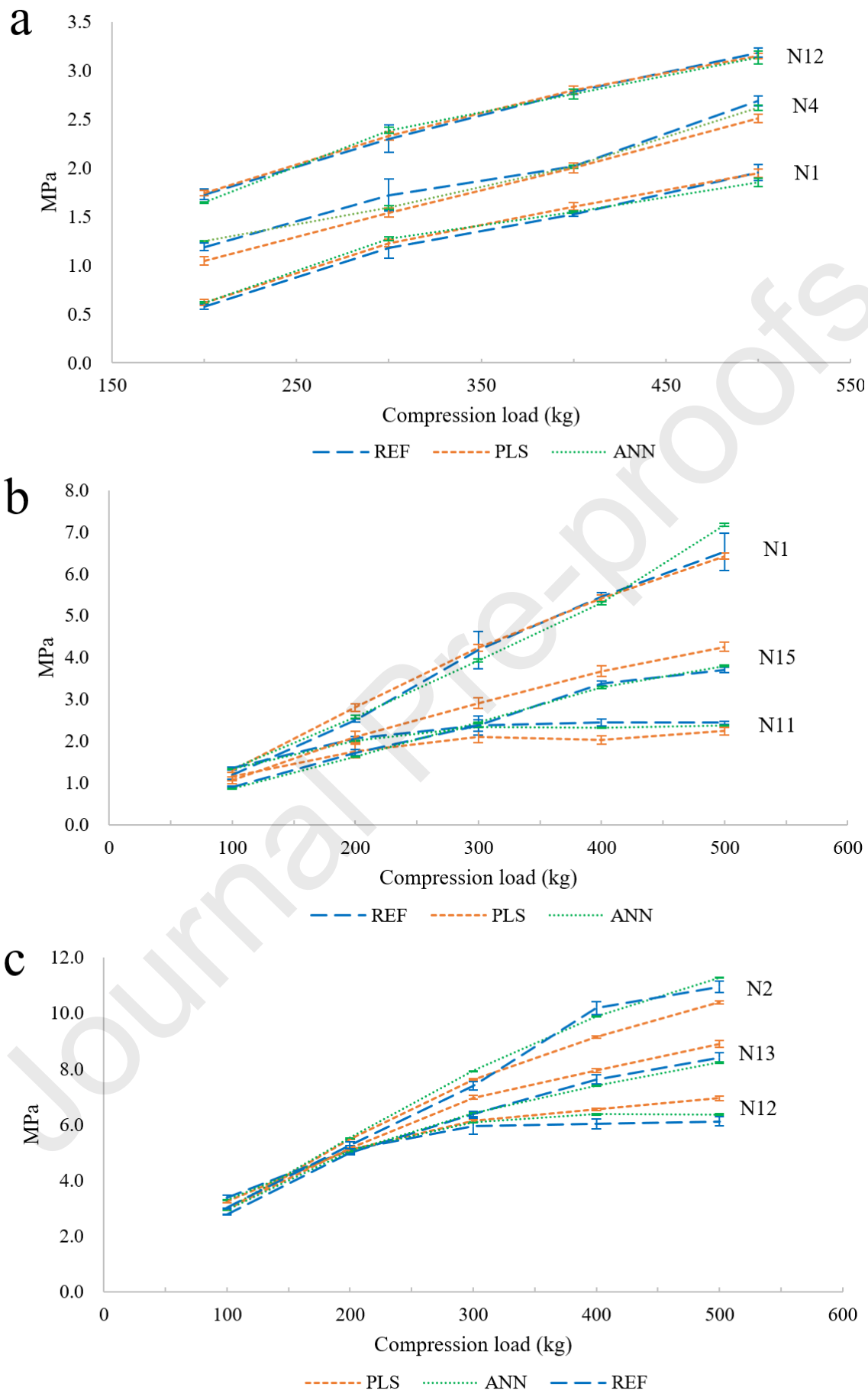

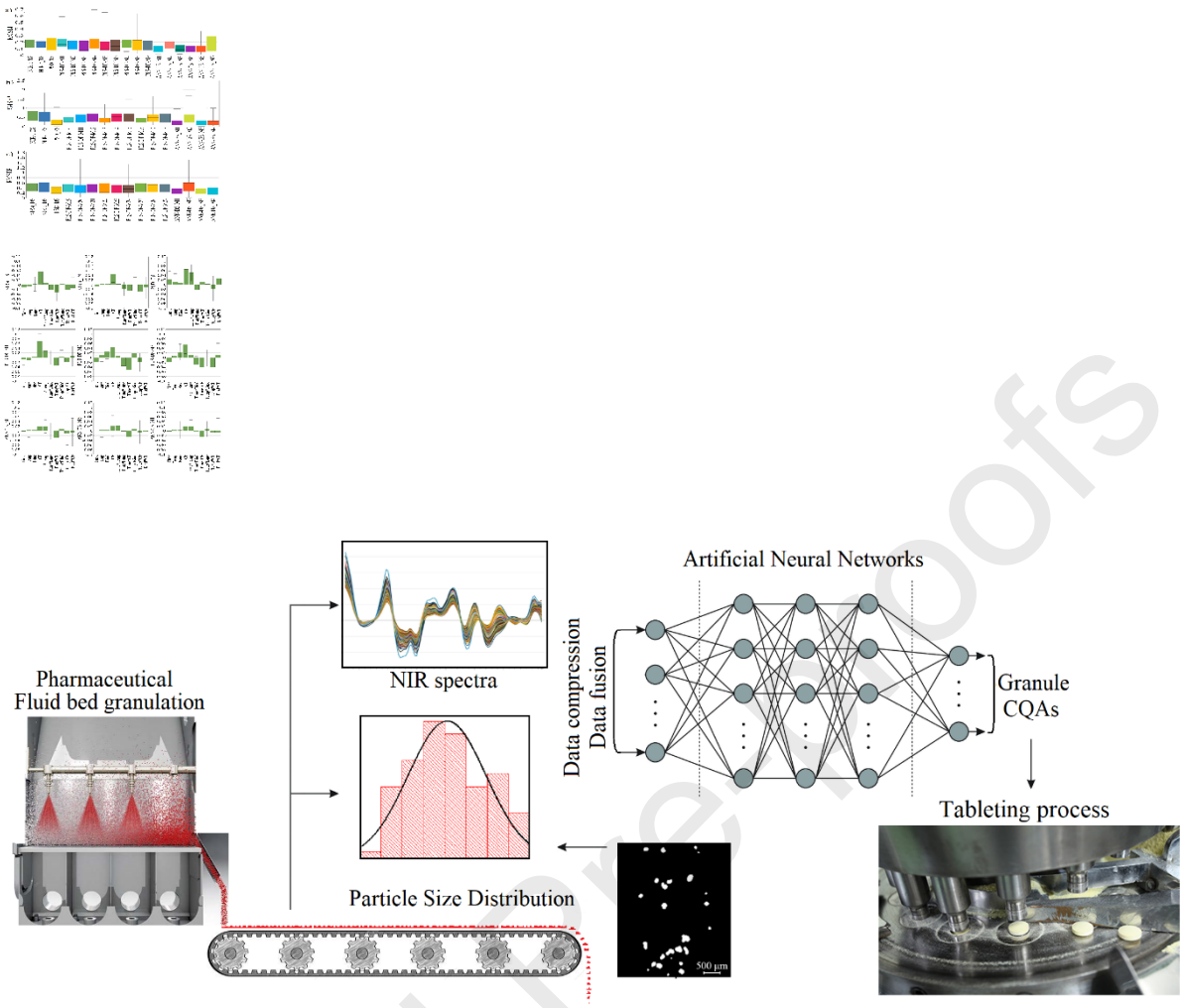


## Author contributions

**Tibor Casian:** Conceptualization, Data curation, Formal analysis, Methodology, Writing - original draft **Brigitta Nagy:** Data curation, Formal analysis, Software, Writing - review & editing **Cristiana Lazurca:** Investigation **Victor Marcu:** Investigation **Erzsébet Orsolya Tőkés:** Investigation **Éva Katalin Kelemen:** Resources **Katalin Zöldi:** Resources **Radu Oprean:** Supervision, Validation **Zsombor Nagy:** Supervision **Ioan Tomuta:** Supervision **Béla Kovács:** Supervision, Methodology, Conceptualization, Writing - review & editing

**Declaration of interests**

☒ The authors declare that they have no known competing financial interests or personal relationships that could have appeared to influence the work reported in this paper.

☐ The authors declare the following financial interests/personal relationships which may be considered as potential competing interests: